

# Mechanical Yield in Amorphous Solids: Spinodal Criticality

Itamar Procaccia

The Weizmann Institute of Science

Rehovot, 76100 Israel

Work with: Giorgio Parisi, Corrado Rainone  
Murari Singh

Paris October 2017

# Glass phenomenology

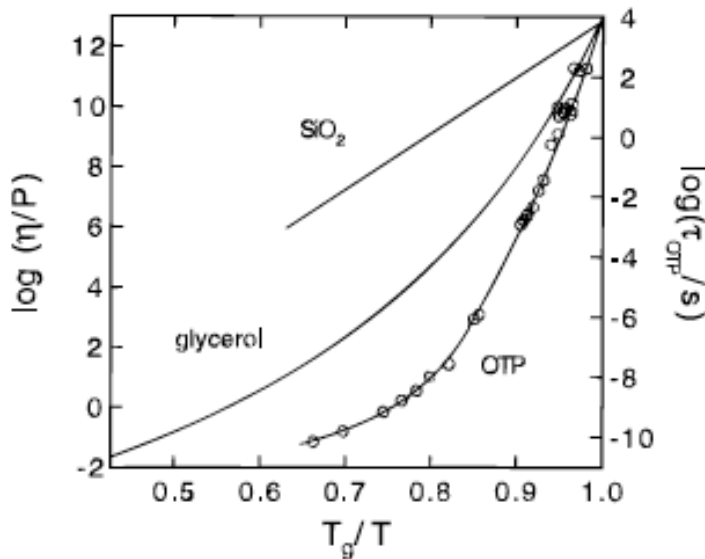
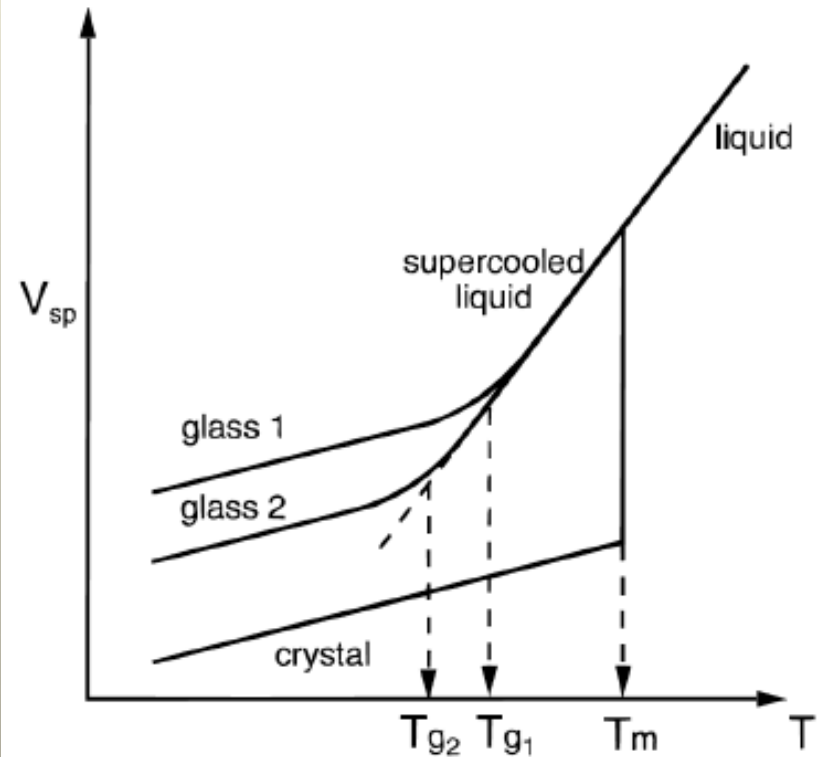
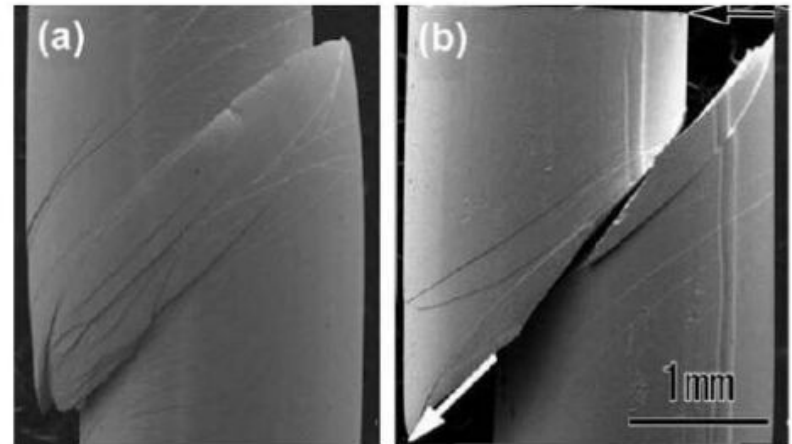


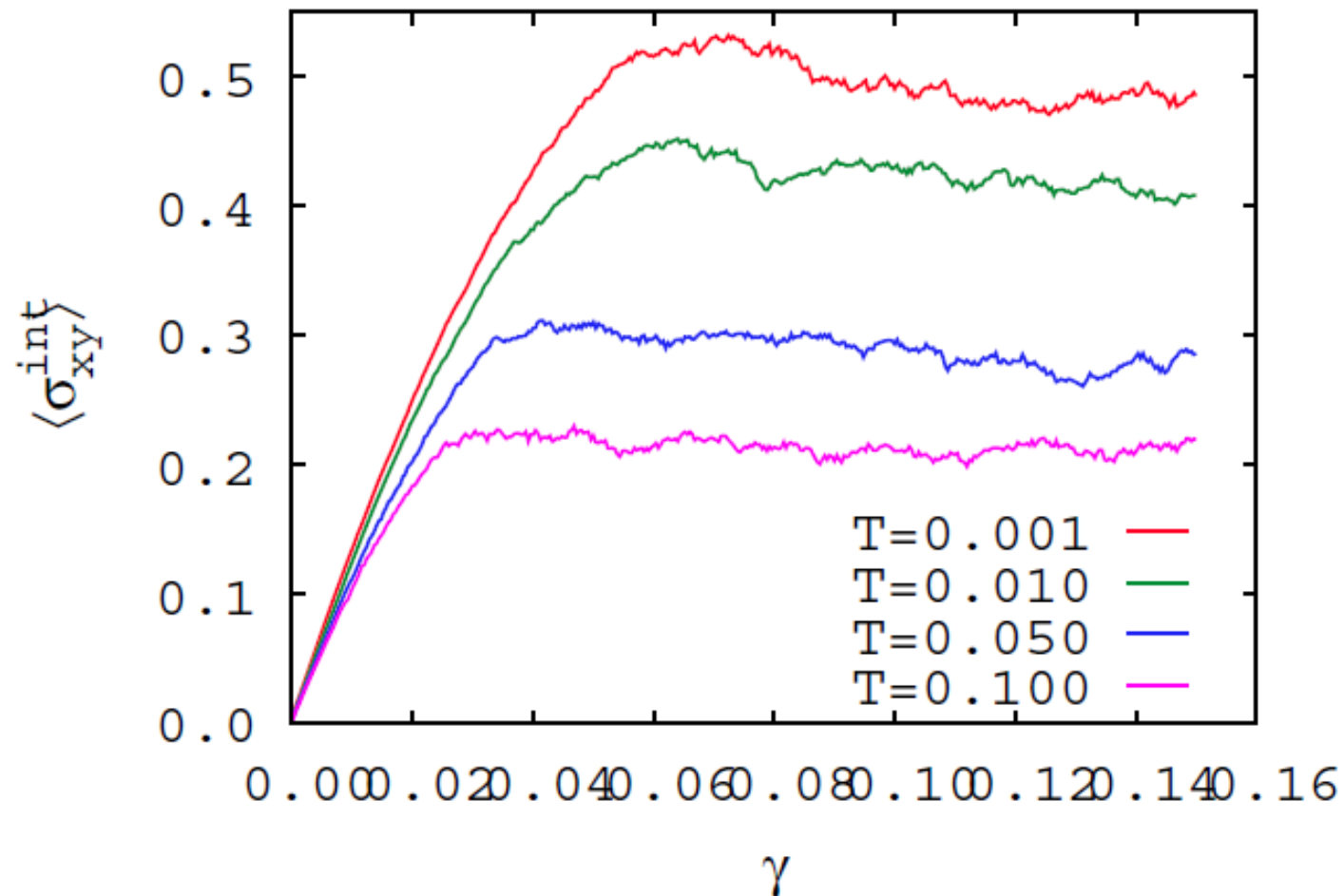
**Figure 2.** Viscosity as a function of reduced inverse temperature for three liquids:  $\text{SiO}_2$ , glycerol, and *o*-terphenyl. Reorientation times are shown for *o*-terphenyl only (○). A nearly Arrhenius temperature dependence for relaxation times and the viscosity is characteristic of *strong* liquids, while *fragile* liquids show quite non-Arrhenius behavior. Data from refs 4–7.



# Mechanical yield in amorphous solids can be catastrophic



Many amorphous solids fail mechanically in the same way!

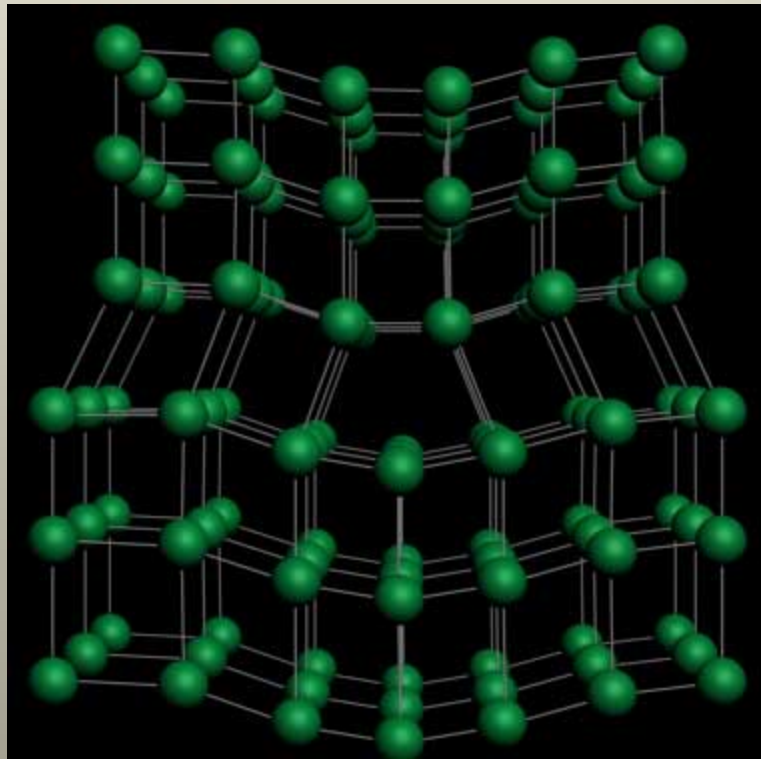


What is the difference in material before and after yield?

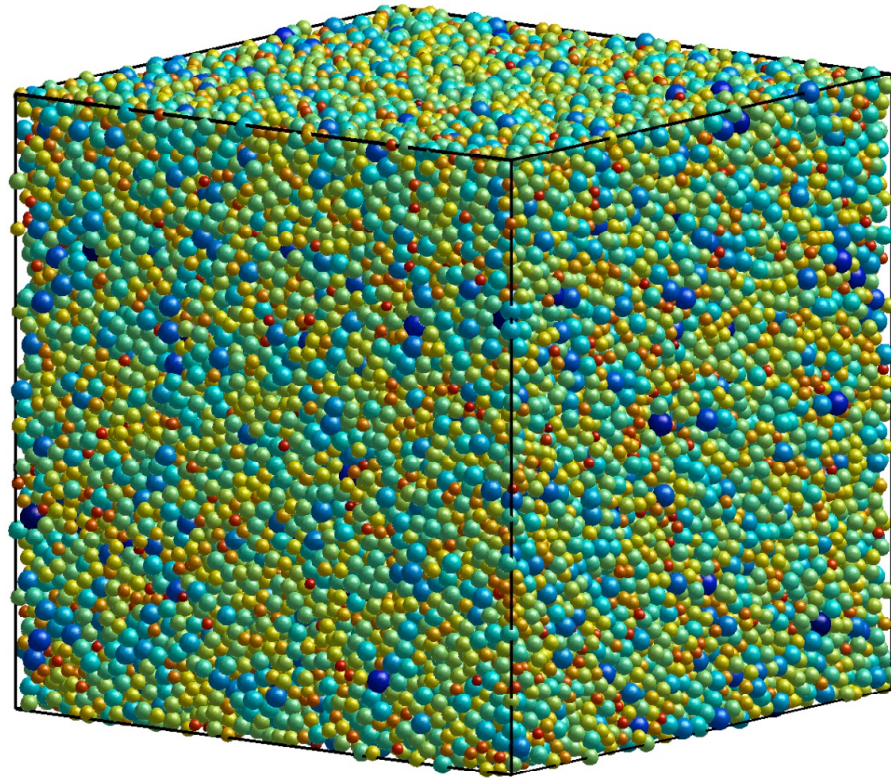
The same basic phenomenology appears irrespective of the microscopic interaction potential!

We are seeking a universal language  
to describe the transition

# Plasticity in crystalline materials



Glasses are disordered like liquids

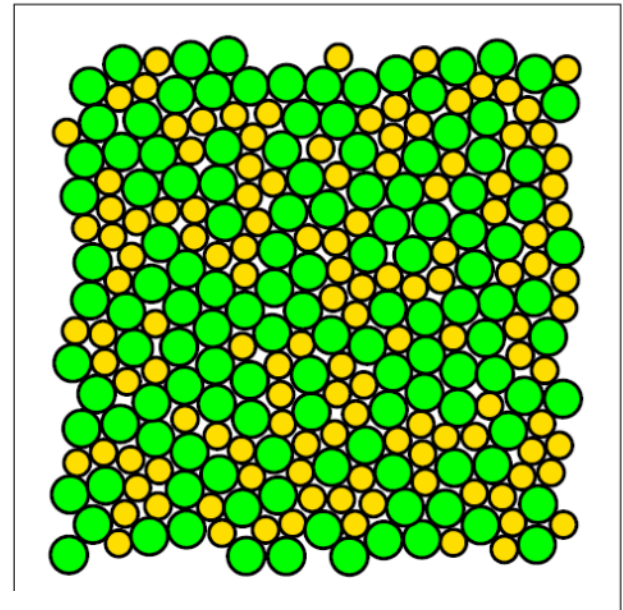


# So what is plasticity in amorphous solids?

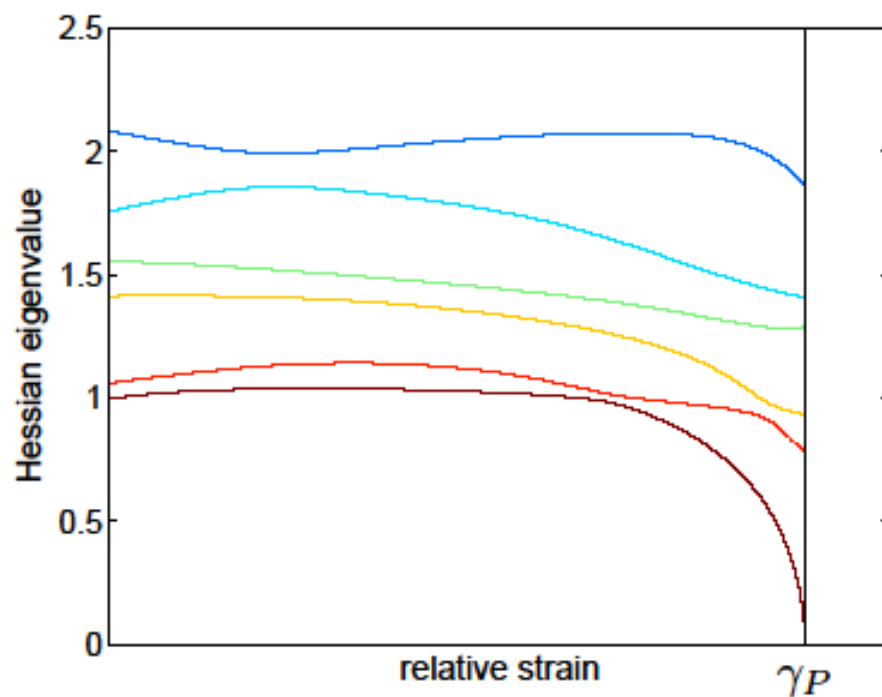
Malandro and Lacks '99; Maloney and Lemaitre '06

$$\mathbf{x}_i \rightarrow \mathbf{J} \cdot \mathbf{x}_i + \mathbf{u}_i$$

$$\frac{d\mathbf{f}_i}{d\gamma} = -\frac{d}{d\gamma} \frac{\partial U}{\partial \mathbf{r}_i} = -\frac{d}{d\gamma} \frac{\partial U}{\partial \mathbf{u}_i} = 0,$$



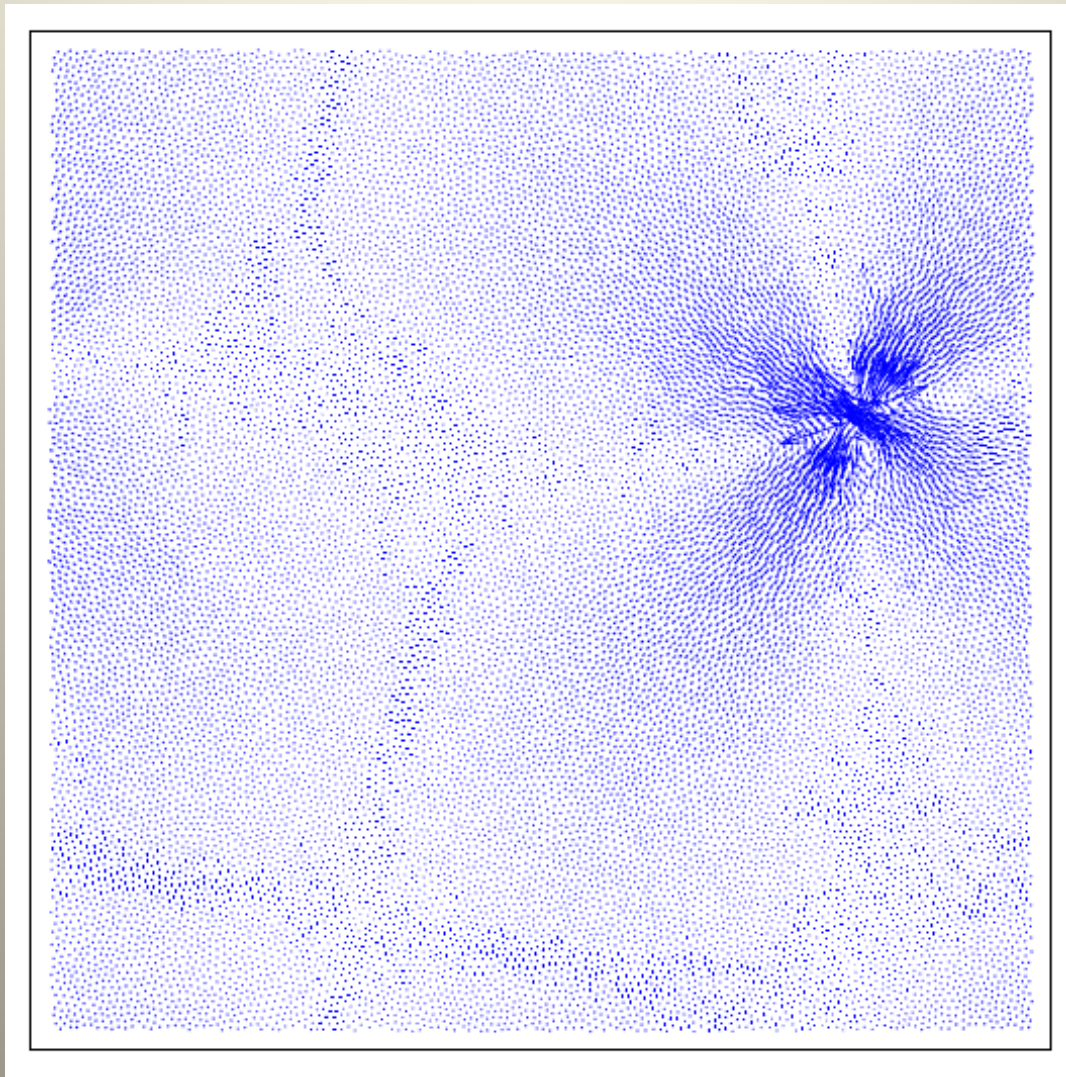
$$\frac{\partial^2 U}{\partial \gamma \partial \mathbf{u}_i} + \frac{\partial^2 U}{\partial \mathbf{u}_j \partial \mathbf{u}_i} \frac{d\mathbf{u}_j}{d\gamma} \equiv \mathbf{\Xi}_i + \mathbf{H}_{ij} \frac{d\mathbf{u}_j}{d\gamma} = 0 .$$



$$\lambda_P \propto \sqrt{\gamma_P - \gamma}.$$

$$\frac{du_i}{d\gamma} = -\mathbf{H}_{ij}^{-1} \mathbf{\Xi}_j = -\sum_k \frac{\psi_j^{(k)} \cdot \mathbf{\Xi}_j}{\lambda_k} \psi_i^{(k)} \approx -\frac{\psi_j^{(P)} \cdot \mathbf{\Xi}_j}{\lambda_P} \psi_i^{(P)},$$

In two dimensions:



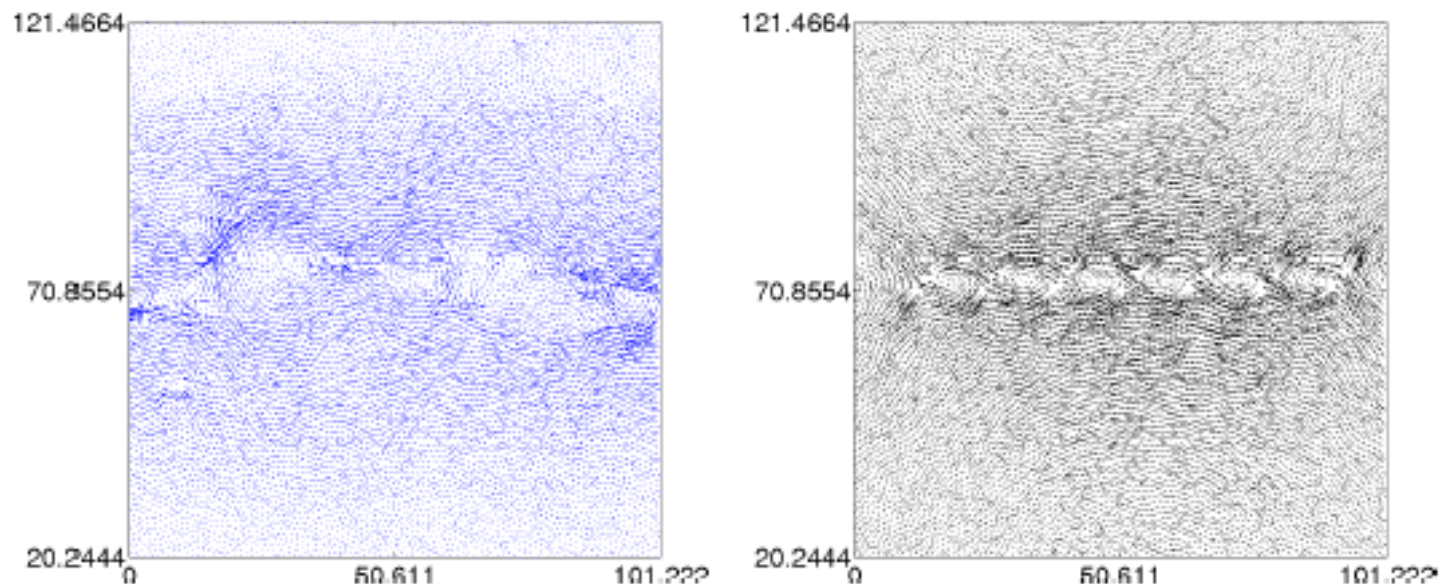


FIG. 4: (Color Online). Left panel: The nonaffine displacement field associated with a plastic instability that results in a shear band. Right panel: the displacement field associated with 7 Eshelby inclusions on a line with equal orientation. Note that in the left panel the quadrupoles are not precisely on a line as a result of the finite boundary conditions and the randomness. In the right panel the series of  $\mathcal{N} = 7$  Eshelby inclusions, each given by Eq. (18) and separated by a distance of 13.158, using the best fit parameters of Fig. 2, have been superimposed to generate the displacement field shown.

# The energetic argument

$$u_{\alpha}^c(\mathbf{X}) = \quad (18)$$

$$\frac{\epsilon^*}{4(1-\nu)} \left(\frac{a}{r}\right)^2 \left[2(1-2\nu) + \left(\frac{a}{r}\right)^2\right] \left[2\hat{n}_{\alpha} \mathbf{n} \cdot \mathbf{X} - X_{\alpha}\right]$$

$$+ \frac{\epsilon^*}{2(1-\nu)} \left(\frac{a}{r}\right)^2 \left[1 - \left(\frac{a}{r}\right)^2\right] \left[\frac{2(\mathbf{n} \cdot \mathbf{X})^2}{r^2} - 1\right] X_{\alpha} .$$

Phys.Rev. Lett., **109** 25502 (2012).

Phys. Rev. E, **87**, 022810 (2013) Phys. Rev. E., **88**, 022310 (2013)

$$E_{mat} \equiv \frac{1}{2} \sigma_{\alpha\beta}^{(\infty)} \epsilon_{\beta\alpha}^{(\infty)} V = V \sigma_{xy}^{(\infty)} \epsilon_{xy}^{(\infty)} = \frac{V \mathcal{E} \gamma^2}{2(1+\nu)}$$

$$E^{\infty} \equiv -\frac{1}{2} \sigma_{\alpha\beta}^{(\infty)} \left( \sum_{i=1}^{\mathcal{N}} \epsilon_{\beta\alpha}^{(*,i)} V_0^{(i)} \right) = -\pi a^2 \sigma_{xy}^{(\infty)} \sum_{i=1}^{\mathcal{N}} \epsilon_{yx}^{(*,i)} = -\frac{\pi a^2 \mathcal{E} \gamma \epsilon^*}{(1+\nu)} \sum_{i=1}^{\mathcal{N}} \hat{n}_x^{(i)} \hat{n}_y^{(i)}$$

$$E_{esh} \equiv -\frac{1}{2} \sum_{i=1}^{\mathcal{N}} \epsilon_{\beta\alpha}^{(*,i)} \sigma_{\alpha\beta}^{(c,i)} V_0^{(i)} + \frac{1}{2} \sum_{i=1}^{\mathcal{N}} \epsilon_{\beta\alpha}^{(*,i)} \sigma_{\alpha\beta}^{(*,i)} V_0^{(i)} = \frac{\pi a^2}{2} \sum_{i=1}^{\mathcal{N}} \left( \sigma_{\alpha\beta}^{(*,i)} - \sigma_{\alpha\beta}^{(c,i)} \right) \epsilon_{\beta\alpha}^{(*,i)}$$

$$E_{inc} \equiv -\frac{1}{2} \sum_{i=1}^{\mathcal{N}} \epsilon_{\beta\alpha}^{(*,i)} V_0^{(i)} \left( \sum_{j \neq i} \sigma_{\alpha\beta}^{(c,j)} (R_{ij}) \right) = -\frac{\pi a^2}{2} \sum_{\langle ij \rangle} \left[ \epsilon_{\beta\alpha}^{(*,i)} \sigma_{\alpha\beta}^{(c,j)} (R_{ij}) + \epsilon_{\beta\alpha}^{(*,j)} \sigma_{\alpha\beta}^{(c,i)} (R_{ij}) \right]$$

$$\frac{E(\rho, \gamma)}{La} = U_p \left[ \left( 1 - \frac{\gamma}{\gamma_Y} \right) a\rho - B(a\rho)^3 + C(a\rho)^5 \right]$$

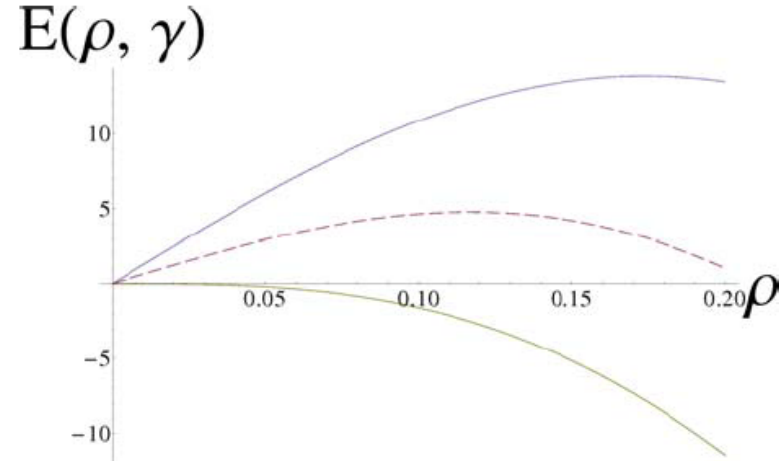


FIG. 1: (Color Online). The total plastic energy Eq. (3) for the creation of an array of quadrupoles with density  $\rho$  for three values of  $\gamma$ :  $\gamma = \gamma_Y - 0.1$  (upper curve),  $\gamma = \gamma_Y - 0.05$  (middle curve), and  $\gamma = \gamma_Y$  (lower curve). In the present case  $\gamma_Y = 0.07$ . To generate this picture we use the measured constants  $\mathcal{E} \approx 37.2$ ,  $\nu \approx 0.31$ ,  $\epsilon^* \approx 0.082$  and  $a = 1.83$ . Finally  $U_p \approx 0.22$ .

$$\gamma_Y \equiv \gamma_Y(T = 0, \dot{\gamma} = 0) \equiv \frac{\epsilon^*}{2(1 - \nu)}.$$

# How to construct an order parameter that will do the job?

Consider two different configurations of a glassy material

$$\{r_i^{(1)}\}_{i=1}^N \text{ and } \{r_i^{(2)}\}_{i=1}^N,$$

$$Q_{12} \equiv \frac{1}{N} \sum_i^N \theta(a - |r_i^{(1)} - r_i^{(2)}|) ,$$

Start with a glass-former in the liquid state at some temperature above the glass transition.

Quench to  $T=0$ .

Heat up to a low temperature (in our case  $T=0.2$ ) much below the glass transition.

Picking up one configuration, randomize the velocities 500 times with Boltzmann weight and quench again to  $T=0$ . This creates one “patch” of configurations.

Repeat and create 100 patches

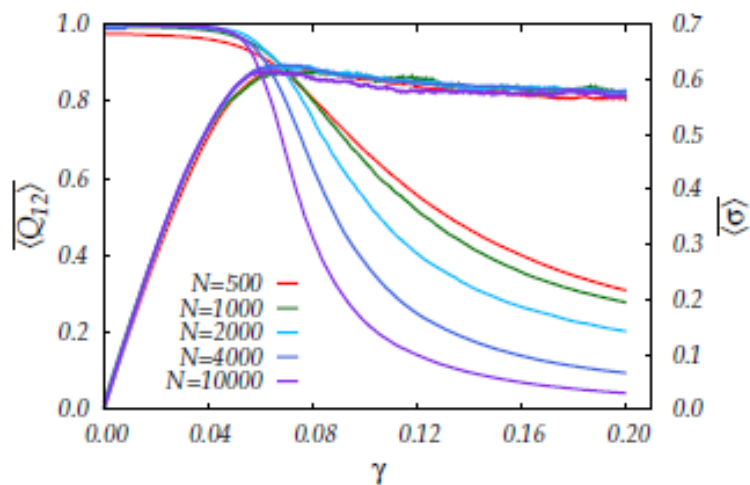


FIG. 6. Demonstrating the sharpening of the transition with the system size.

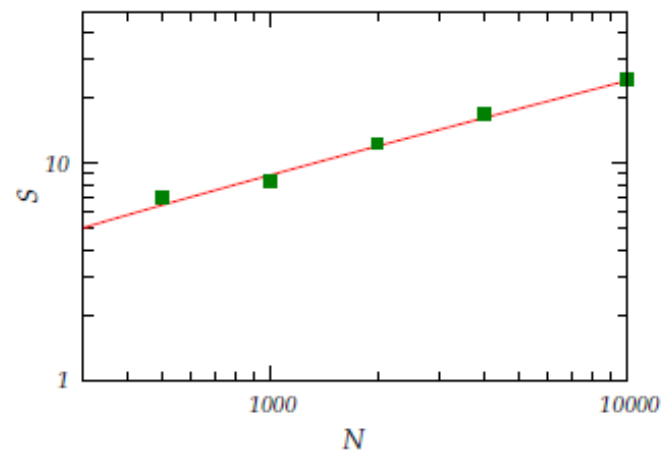
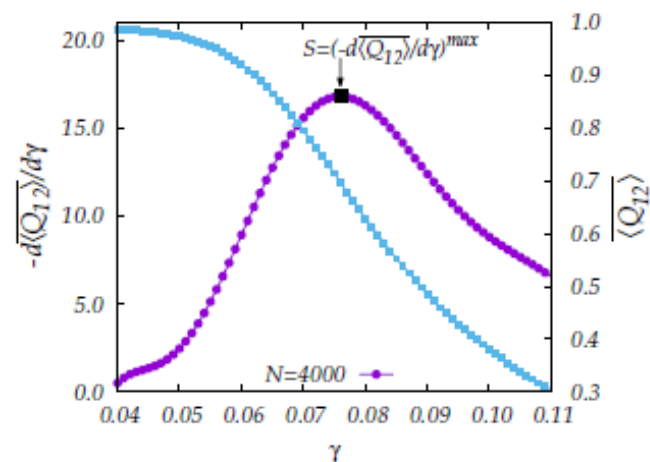


FIG. 7. Upper panel: A typical graph of  $\overline{\langle Q_{12} \rangle}$  as a function of  $\gamma$  (here for  $N = 4000$  (right scale) and the slope of the same function (left scale). Lower panel: The maximal slope of the function  $\overline{\langle Q_{12} \rangle}(\gamma)$  as a function of system size.

## Yield is a “stressed ergodization”

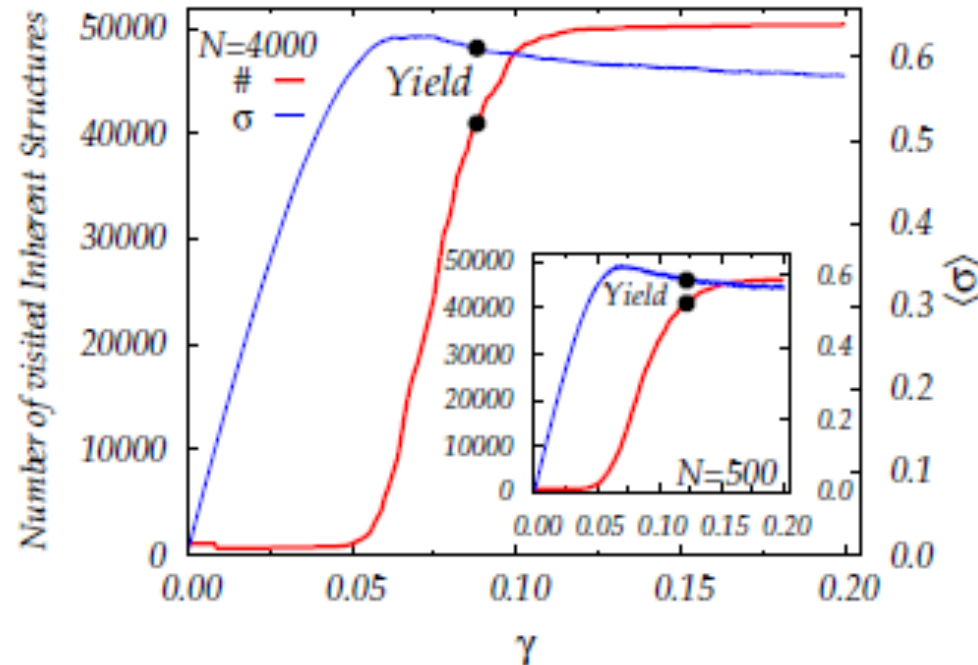


FIG. 5: The number of configurations which pass below the threshold value  $Q_{12} = 0.8$  of the overlap order parameter as a function of the strain  $\gamma$  for  $N = 4000$ . In the onset we show the same test for  $N = 500$ . The conclusion is that *all the configurations* lose overlap with the initial configuration in the vicinity of the yield point  $\gamma_Y$

Since we have enough initial configurations, we can consider the probability of the order parameter, averaged over the realizations

3

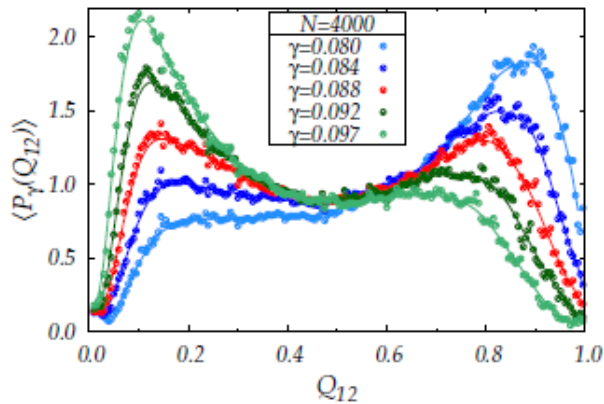


FIG. 4: The probability distribution function  $\langle P_\gamma(Q_{12}) \rangle$  in the vicinity of the critical point  $\gamma_Y = 0.088$

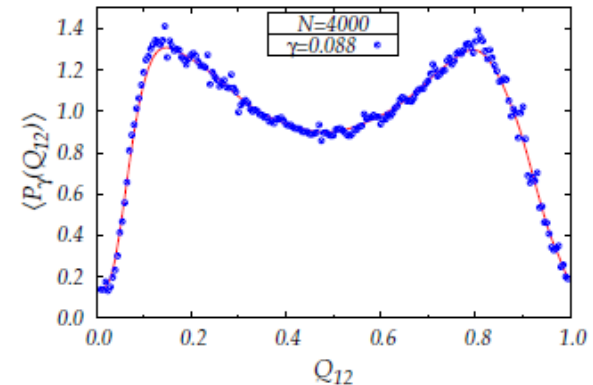


FIG. 3: The probability distribution function  $P_\gamma(Q_{12})$  at  $\gamma_Y = 0.088$  averaged over 100 initial configurations each of which has 500 different realizations to obtain  $\langle P_\gamma(Q_{12}) \rangle$ . At this value of the strain the pdf has two peaks of equal heights. We identify this value of  $\gamma$  as the point of the phase transition.

G. Parisi, IP, C. Rainone, M. Singh  
PNAS June 2017

$$Q_{ab}(\mathbf{r}) \equiv \sum_{i=1}^N \theta(\ell - |\mathbf{r}_i^a - \mathbf{r}_i^b|) \delta(\mathbf{r} - \mathbf{r}_i^a) ,$$

$$G_L(\mathbf{r}) = 2G_R(\mathbf{r}) - \Gamma_2(\mathbf{r}), \quad (3)$$

with the definitions

$$G_R(\mathbf{r}) \equiv \overline{\langle Q_{ab}(\mathbf{r}) Q_{ab}(0) \rangle} - 2 \overline{\langle Q_{ab}(\mathbf{r}) Q_{ac}(0) \rangle} \quad (4)$$

$$+ \overline{\langle Q_{ab}(\mathbf{r}) \rangle} \overline{\langle Q_{cd}(0) \rangle},$$

$$\Gamma_2(\mathbf{r}) \equiv \overline{\langle Q_{ab}(\mathbf{r}) Q_{ab}(0) \rangle} - \overline{\langle Q_{ab}(\mathbf{r}) \rangle} \overline{\langle Q_{ab}(0) \rangle} . \quad (5)$$

$$\chi_{G_L}(\gamma) \equiv \int d^2x \, G_L(x, y; \gamma) .$$

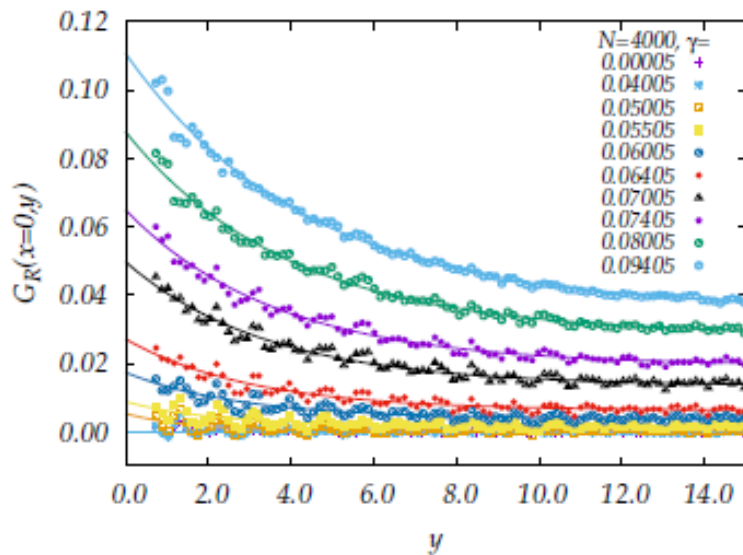


FIG. 2. The function  $G_R(x=0, y; \gamma)$  for various values of  $\gamma$  from  $5 \times 10^{-5}$  to 0.09405. Note the increase in the overall amplitude of the correlator as well as the increase in the correlation length. The lines through the data are the fit function Eq. (10).

$$\xi \approx (\gamma_c - \gamma)^{-\nu}, \quad \nu \approx 2.4 \pm 0.35.$$

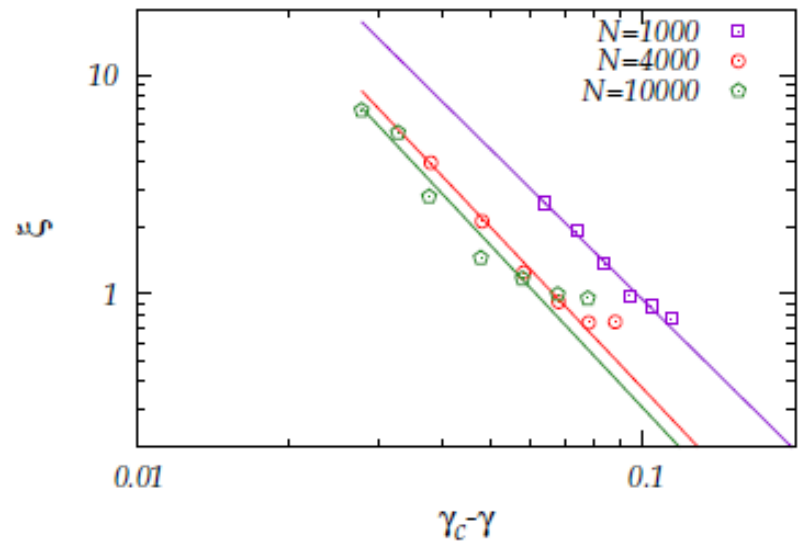
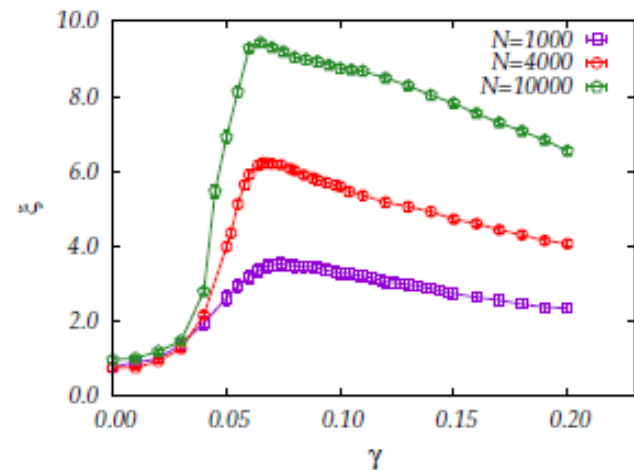


FIG. 16. Upper panel: the correlation length  $\xi$  read from an exponential fit to the  $x$  and  $y$  projection of the correlation function  $\Gamma_2(x, y)$  for three values of the system size. Lower panel: the dependence of the correlation length  $\xi$  on  $\gamma - \gamma_c$ .

Note that in thermal systems a spinodal point cannot be stabilized!

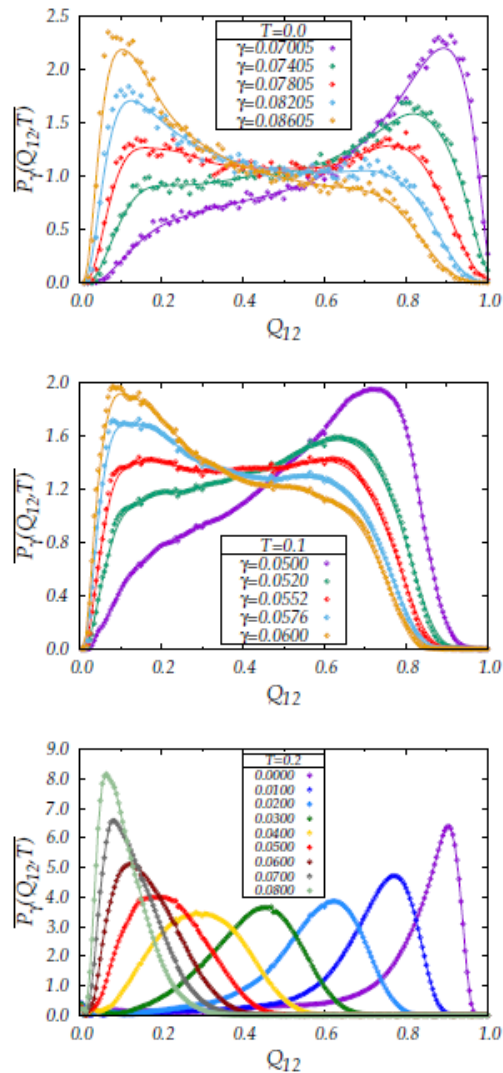


FIG. 18. The dependence of  $\overline{P}_\gamma(Q_{12}, T)$  on  $\gamma$  for three different temperatures  $T = 0, 0.1, 0.2$ .

Thank you!

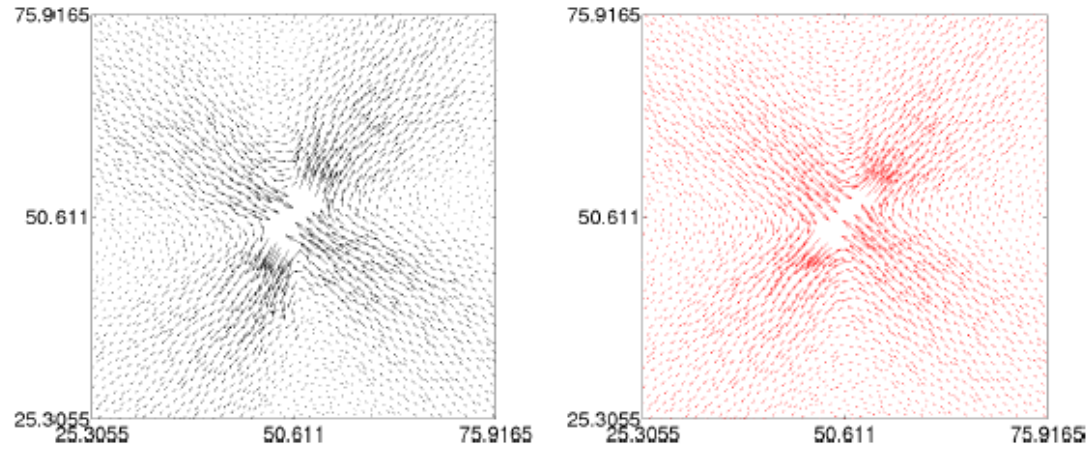


FIG. 2: (Color Online). Left panel: the localization of the non-affine displacement onto a quadrupolar structure which is modeled by an Eshelby inclusion, see right panel. Right panel: the displacement field associated with a single Eshelby circular inclusion of radius  $a$ , see text. The best fit parameters are  $a \approx 2.5$  and  $\epsilon^* \approx 0.1$ . To remove the effect of boundary conditions, the best fit is generated on a smaller box of size  $(x, y) \in [25.30, 75.92]$

$$\begin{aligned}
 u_{\alpha}^c(\mathbf{X}) = & \quad (18) \\
 & \frac{\epsilon^*}{4(1-\nu)} \left(\frac{a}{r}\right)^2 \left[2(1-2\nu) + \left(\frac{a}{r}\right)^2\right] \left[2\hat{n}_{\alpha} \mathbf{n} \cdot \mathbf{X} - X_{\alpha}\right] \\
 & + \frac{\epsilon^*}{2(1-\nu)} \left(\frac{a}{r}\right)^2 \left[1 - \left(\frac{a}{r}\right)^2\right] \left[\frac{2(\mathbf{n} \cdot \mathbf{X})^2}{r^2} - 1\right] X_{\alpha} .
 \end{aligned}$$

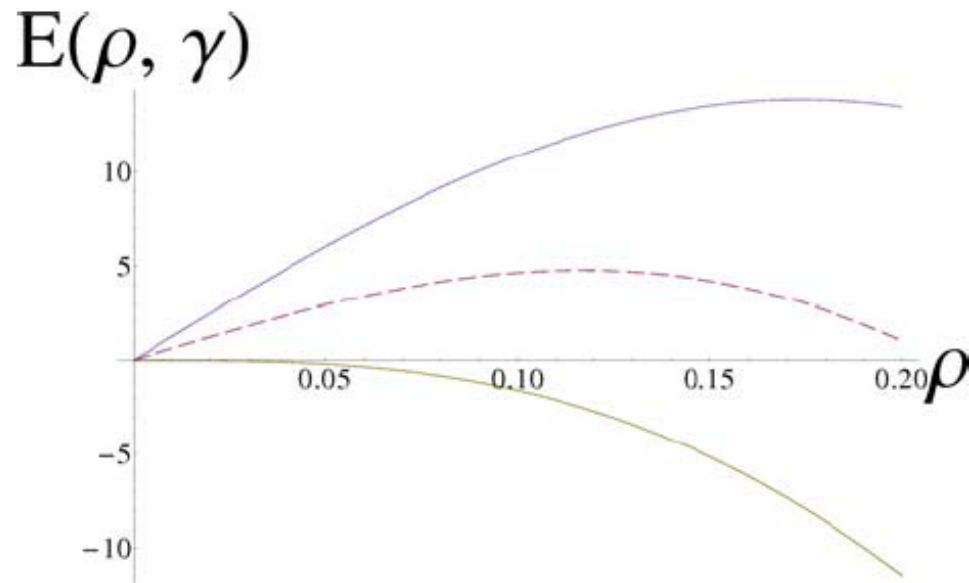
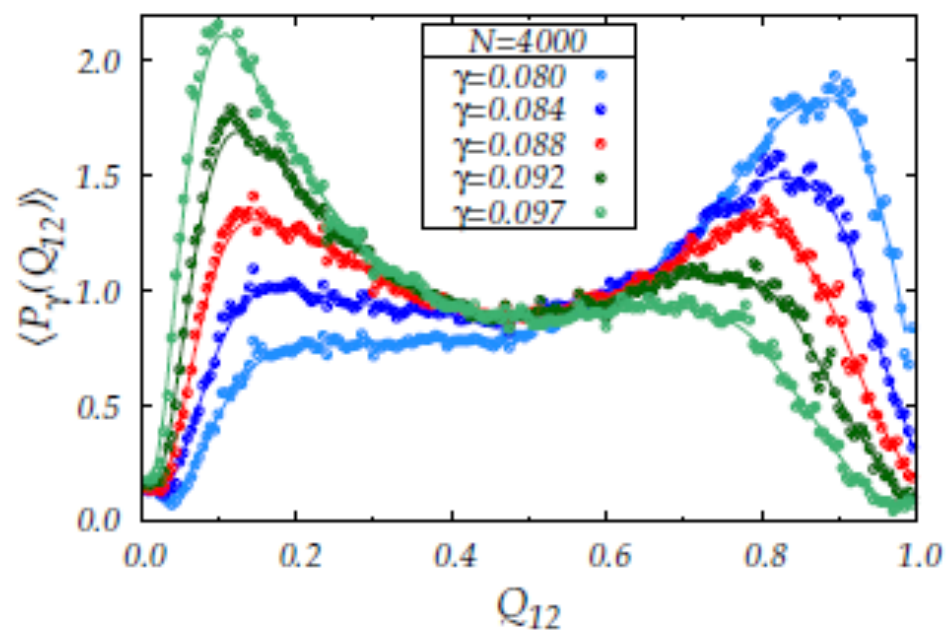
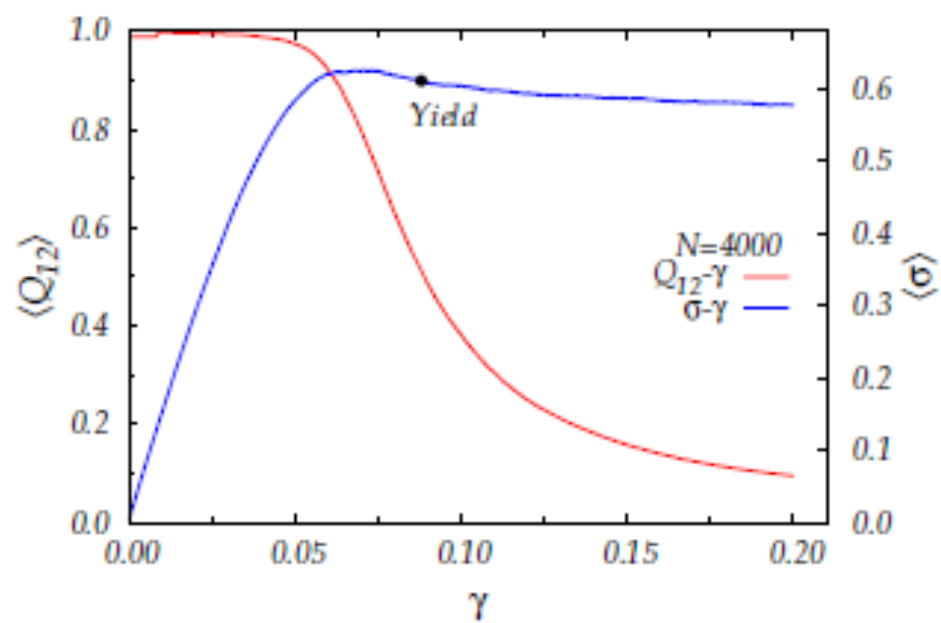


FIG. 1: (Color Online). The total plastic energy Eq. (3) for the creation of an array of quadrupoles with density  $\rho$  for three values of  $\gamma$ :  $\gamma = \gamma_Y - 0.1$  (upper curve),  $\gamma = \gamma_Y - 0.05$  (middle curve), and  $\gamma = \gamma_Y$  (lower curve). In the present case  $\gamma_Y = 0.07$ . To generate this picture we use the measured constants  $\mathcal{E} \approx 37.2$ ,  $\nu \approx 0.31$ ,  $\epsilon^* \approx 0.082$  and  $a = 1.83$ . Finally  $U_p \approx 0.22$ .

*R. Dasgupta, H. G. E. Hentschel and I. Procaccia,*  
*Phys.Rev. Lett.,***109** 25502 (2012)

*Ashwin J., O. Gendelman, I. Procaccia, C. Shor,*  
*Phys. Rev. E.,* 88, 022310 (2013).



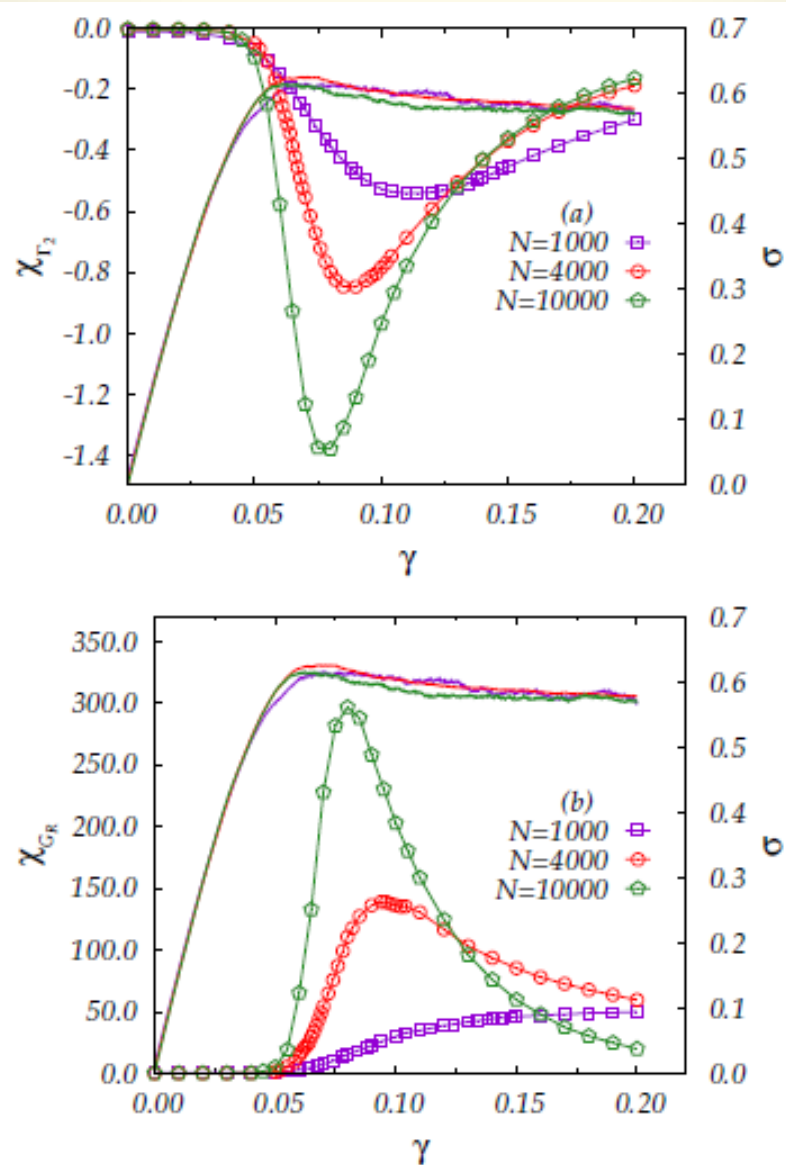


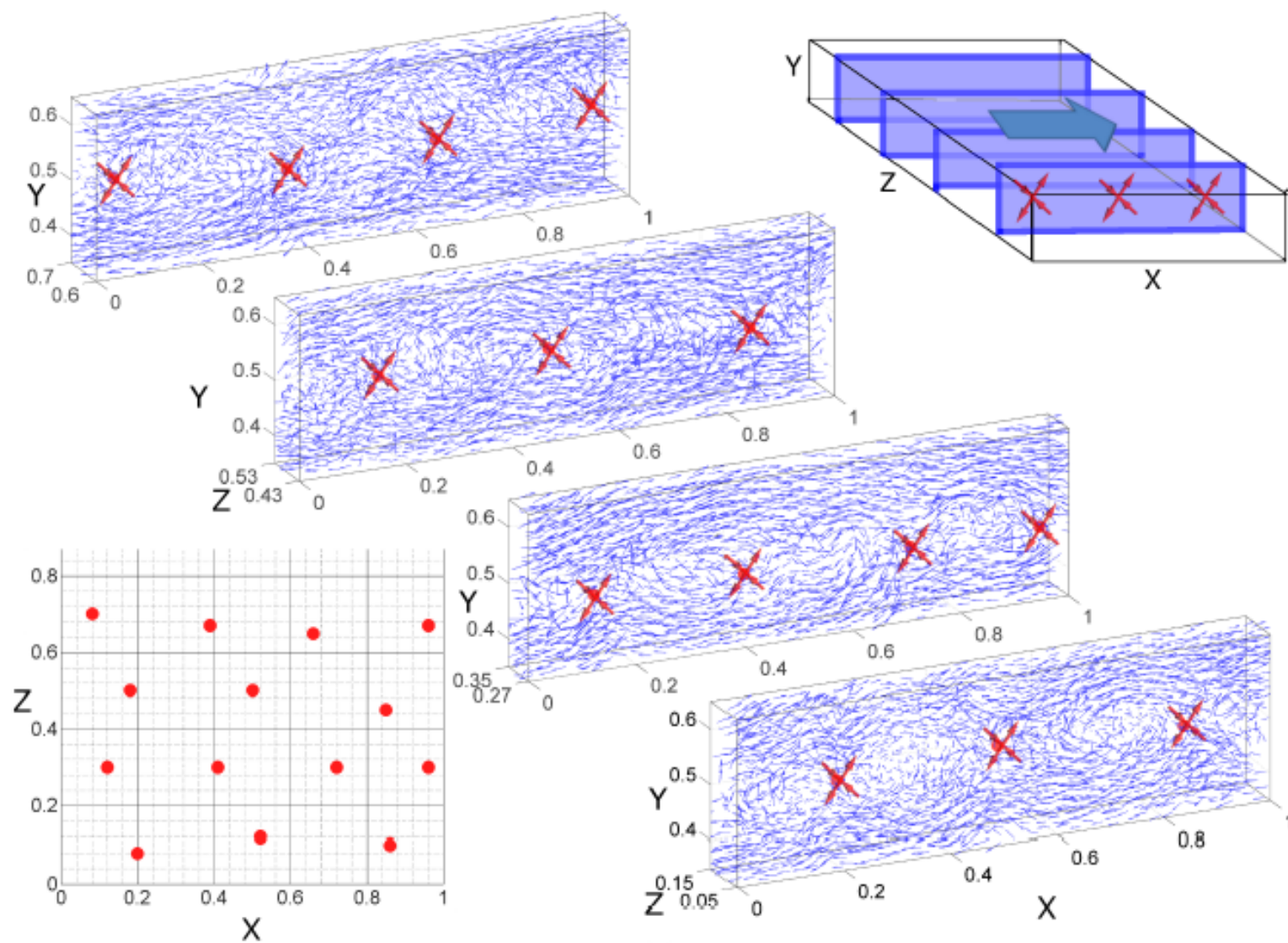
FIG. 1. The susceptibilities  $\chi_{r_2}$  (upper panel) and  $\chi_{G_R}$  (lower panel) as a function of  $\gamma$  for the three systems sizes available. Superimposed are the stress vs. strain curves for comparison. The color code is violet for  $N = 1000$ , red for 4000 and green for 10000.

# Generalization to 3 dimensions

An Eshelby circle generalizes to an Eshelby sphere  
but in fact remains 2-dimensional!

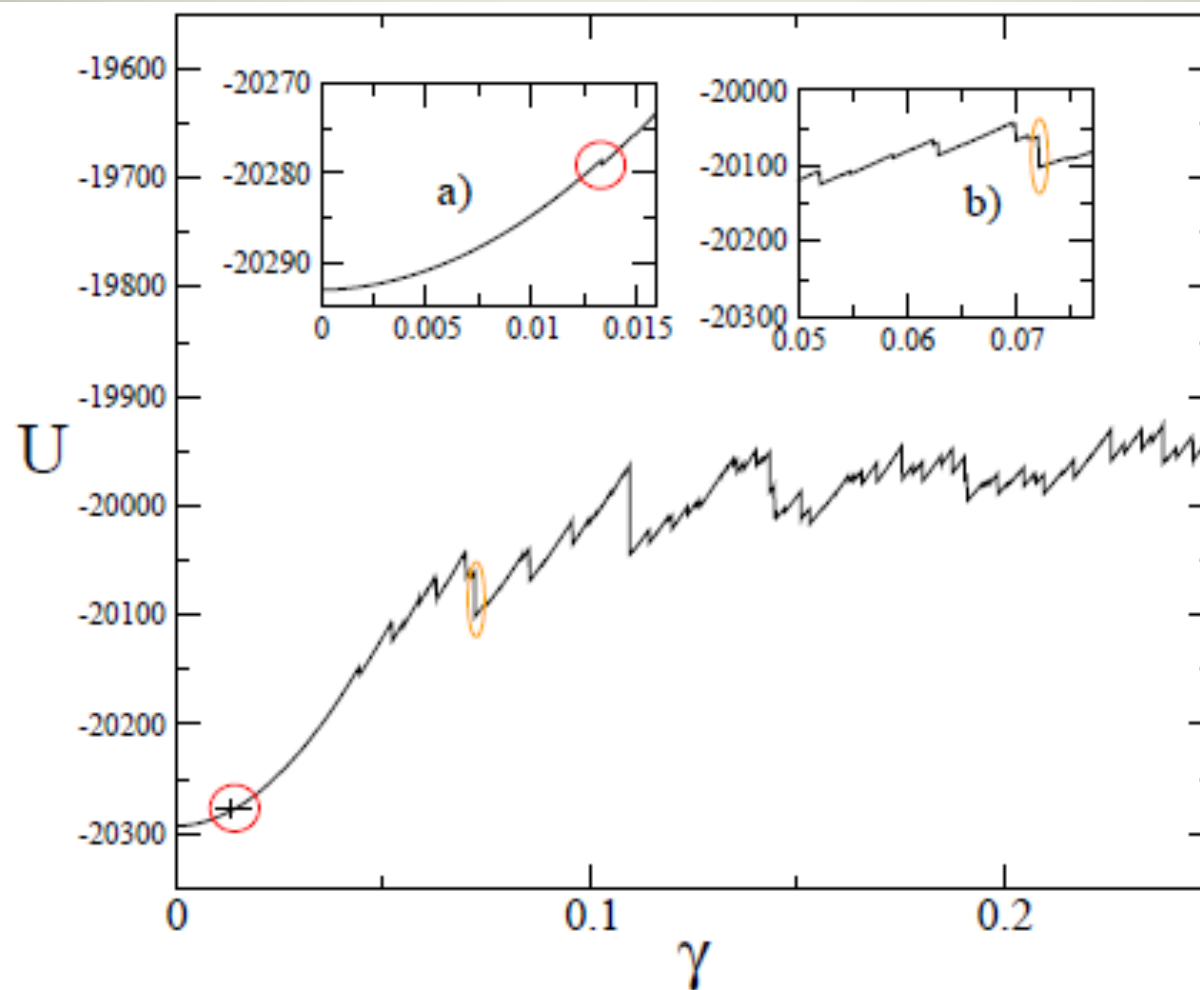
An line of Eshelby quadruoples generalizes to a plane of  
Eshelby ellipsoids

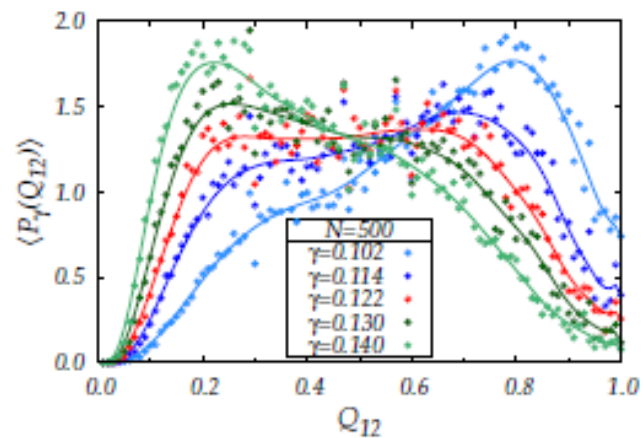
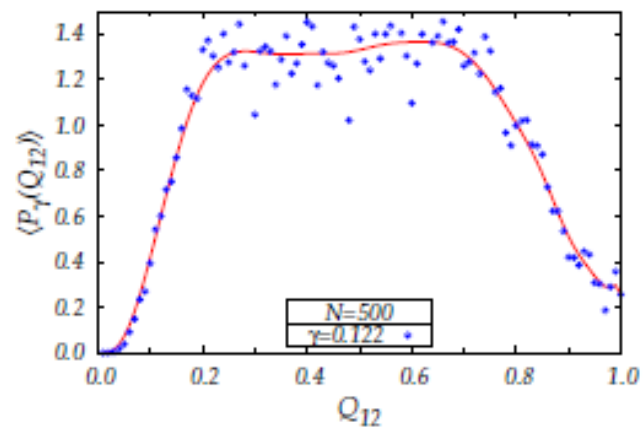
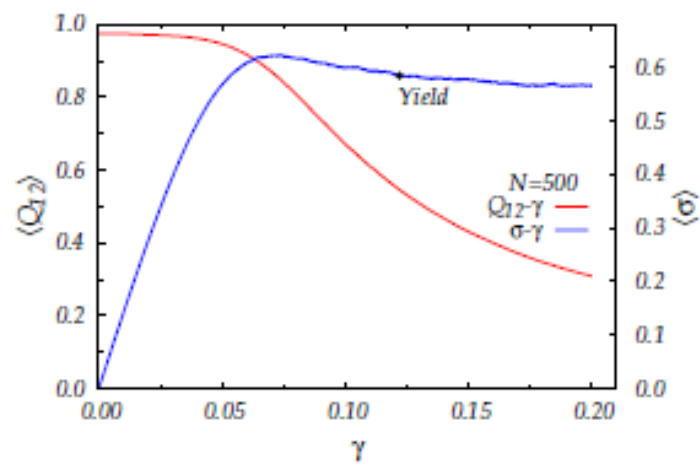
The calculation predicts that the minimal energy arrangement  
is for quadrupoles living on a triangular lattice on the  
localization plane



Thank you!

What is the difference between the state of matter before and after yield?





$$N^{-1/3}$$

We know that the energy drops in plastic events before yield are “small”, scaling like  $N^0$  .

We also know that after the yield the energy drops in the plastic events are “large”, scaling like  $N^{1/3}$  .